

**Magnetic Coupling between the Interior and the Atmosphere of the Sun, “Centenary Commemoration of the discovery of the Evershed Effect”, IIA, Bangalore, India, 2 - 5 December 2008**

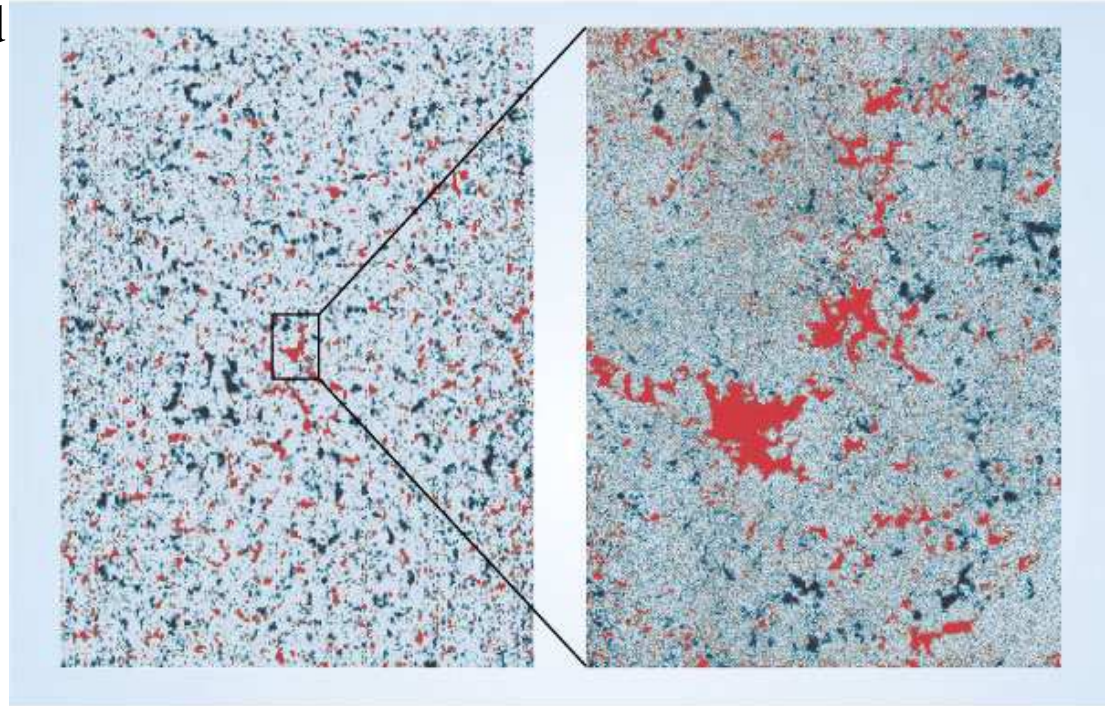
# **Probability distribution functions to represent the solar surface magnetic fields**

**M. Sampurna**

Indian Institute of Astrophysics, Bangalore 560 034, India.

# Observational motivation for the Prob. Dist<sup>n</sup> Fn<sup>s</sup> (PDFs)

- ★ The magnetic fields in the so called “voids” are shown to be actually turbulent using modeling of Hanle effect (Trujillo Bueno et al. 2004)
- ★ Turbulent eddies are shown to be formed by magneto-convection (see eg., Stein & Nordlund 2006), through numerical simulations.



Magnetogram showing opposite polarity (red and blue patches) regions separated by grey voids (“turbulent” fields). Courtesy : Stenflo (2004)

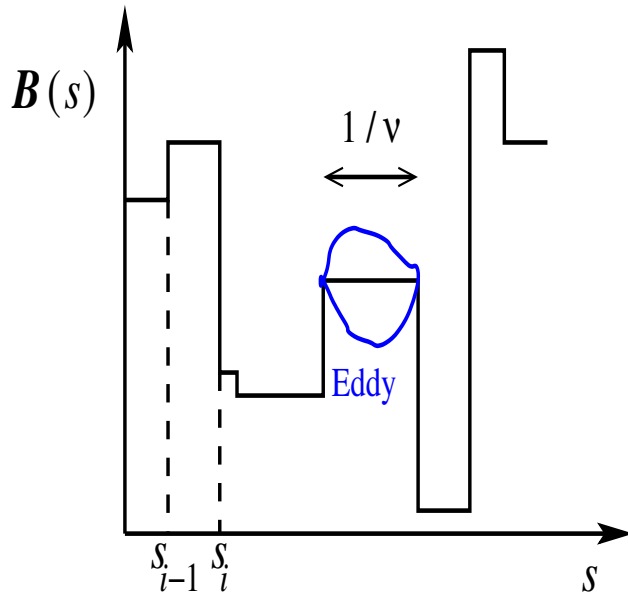
- ★ The size distribution of the eddies are  $\ll$  spatial resolution scale of the present day instruments (0.2”).  $\therefore$  Indirect proof for the “existence of eddies” is necessary.
- ★ Observed Stokes profiles are ‘always’ averaged quantities over space, time and magnetic field.
- ★ The purpose of modeling or simulation is to “extract the scale of turbulence” (size distribution of eddies).

# Magnetic turbulence/ historical background

- ★ The effect of **micro-turbulent** magnetic field on **Zeeman absorption coefficients** was considered long back by **Dolginov & Pavlov (1972)**, and **Domke & Pavlov (1979)**.
- ★ The *first formulation* of Zeeman line radiative transfer in the **micro**, and also **macro-turbulent** limits was due to **Stenflo (1971, 1973)**.
- ★ **MISMA** hypothesis of **Sánchez Almeida et al. (1996)** is based on the idea of ‘**micro-turbulence**’. MISMA is a useful tool in magnetic field diagnostics.
- ★ A theory of Rad. Transf. in **meso-turbulent regime** :- **Landi Degl’Innocenti (1994)**.
- ★ A more **general theory** of Zeeman turbulence and Rad. Transf. is developed in **Frisch, Sampoorna, & Nagendra (2006)**; also **Sampoorna et al. (2007, 2008a, 2008b)**.
- ★ Recently **Carroll & Staude (2003, 2005, 2006)**, and **Carroll & Kopf (2007)**, have taken **an approach similar to ours**, and tried to model **photospheric turbulent fields**.
- ★ It is well known that “**Probability Distribution Functions (PDFs)**” can be used to mathematically represent the **randomness of the field variables** ( $B, \theta_B, \phi_B$ ).
- ★ In this talk I highlight the **importance of PDFs** in **Zeeman line profile computations**.

# A model for the random fields

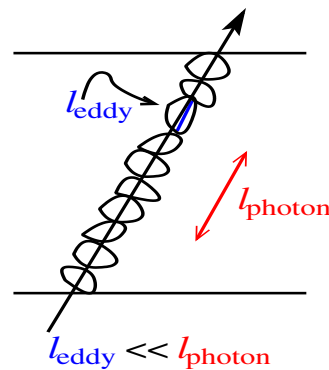
★ We express fluctuations through a Kubo-Anderson process (KAP). It describes the magnetic atmosphere in terms of “eddies”.



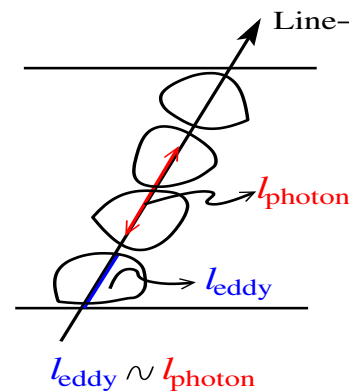
- ▶ In each eddy,  $B$  remains constant & takes “random values” according to a PDF.
- ▶ Further,  $B$  “jumps” at the boundaries of the eddies.
- ▶  $s_i$  are jumping points distributed according to Poisson law.
- ▶ If  $\nu$  = the number of jumps/unit optical depth, then “correlation length”  $\simeq$  mean eddy size ( $l_{\text{eddy}}$ ) =  $1/\nu$ .

2 length scales are involved

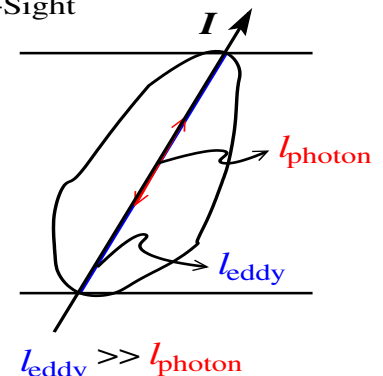
1. Rad. transfer length scale  
 $\simeq$  photon mean free path
2. Turb. length scale  
 $\simeq$  mean eddy size itself



Micro-turbulence  
 $\langle \Phi \rangle$



Meso-turbulence  
 $\langle ? \rangle$



Macro-turbulence  
 $\langle I \rangle$

▶  $\nu \rightarrow 0$  : macro ;       $\nu \rightarrow \infty$  : micro ;       $\langle \rangle$  denote the “mean”

# Mean residual emergent Stokes parameters

★ We consider Residual emergent Stokes parameters :

$$\mathbf{r}(\tau_c = 0) = \frac{1}{C_1} [\mathbf{I}_c(0) - \mathbf{I}(0)]; \quad \mathbf{I}_c(0) = (C_0 + C_1)\mathbf{U}.$$

★ Using KAP in a ME model, we compute the mean values in case of meso-turbulence

$$\langle \mathbf{r}(0) \rangle_{\text{KAP}} = (1 + \nu) \mathbf{R}_{\text{macro}} \left( \frac{\beta}{1 + \nu} \Phi \right) \left[ \mathbf{E} + \nu \mathbf{R}_{\text{macro}} \left( \frac{\beta}{1 + \nu} \Phi \right) \right]^{-1} \mathbf{U},$$

$\beta = k_L/k_c =$  line strength,  $\Phi =$  absorption matrix,  $(1/\nu) =$  correlation length, and

$$\mathbf{R}_{\text{macro}} \left( \frac{\beta}{1 + \nu} \Phi \right) = \left\langle \frac{\beta}{1 + \nu} \Phi \left[ \mathbf{E} + \frac{\beta}{1 + \nu} \Phi \right]^{-1} \right\rangle_{\text{PDF}},$$

★ Rad. Transf. in turbulent media is computationally difficult because of  $\langle \rangle_{\text{PDF}}$  !

★ Analytic simplification of the problem is possible only in micro-turbulent limit.

$$\langle \mathbf{r}(0) \rangle_{\text{micro}} = \beta \underbrace{\langle \Phi \rangle}_{\text{micro}} [\mathbf{E} + \beta \langle \Phi \rangle]^{-1} \mathbf{U}, \quad \langle \mathbf{r}(0) \rangle_{\text{macro}} = \underbrace{\langle \beta \Phi [\mathbf{E} + \beta \Phi]^{-1} \rangle}_{\text{macro}} \mathbf{U}.$$

# Discussion on PDFs in this Talk

I. **Scalar PDFs**  $\Rightarrow$  only **field strength** fluctuates

(eg., Voigt, and stretched exponential)

$\longrightarrow$  **Symmetric** PDFs (zero NET flux)

$\longrightarrow$  **Asymmetric** PDFs (non-zero net flux)

II. **Angular PDFs**  $\Rightarrow$  Fluctuations of **orientation** only

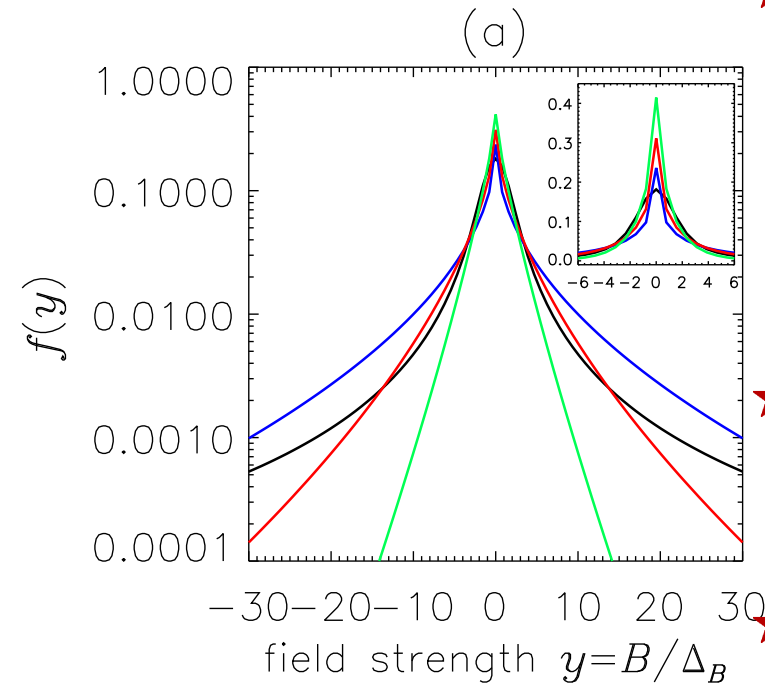
(eg., **Power law**)

III. **Vector PDFs**  $\Rightarrow$  All the variables ( $B, \theta_B, \phi_B$ ) fluctuate

$\longrightarrow$  combination of **Voigt and Power law**

$\longrightarrow$  combination of **Stretched Exp. and Power law**

# Symmetric scalar PDFs (zero net flux)



Voigt and Stretched exponential PDFs

Black line:  $f(y) = P_{\text{Voigt}}(y, a_B = 1.5)$

Blue line:  $f(y) = P_{\text{SE}}(y)$  with  $k = 0.5$

Red line:  $f(y) = P_{\text{SE}}(y)$  with  $k = 0.6$

Green line:  $P_{\text{SE}}(y)$  with  $k = 0.8$

Inset shows a magnified view of the core region of the PDF.

- ★ Stenflo & Holzreuter (2003) deduce a Voigt like PDF from high-resolution La Palma & MDI magnetograms :

$$P_{\text{Voigt}}\left(\frac{B}{\Delta_B}, a_B\right) = \frac{a_B}{\pi^{3/2}} \int_{-\infty}^{+\infty} \frac{e^{-(B_1/\Delta_B)^2}}{[(B - B_1)/\Delta_B]^2 + a_B^2} \frac{dB_1}{\Delta_B},$$

$\Delta_B \rightarrow$  magnetic width,  $a_B \rightarrow$  magnetic damping parameter.

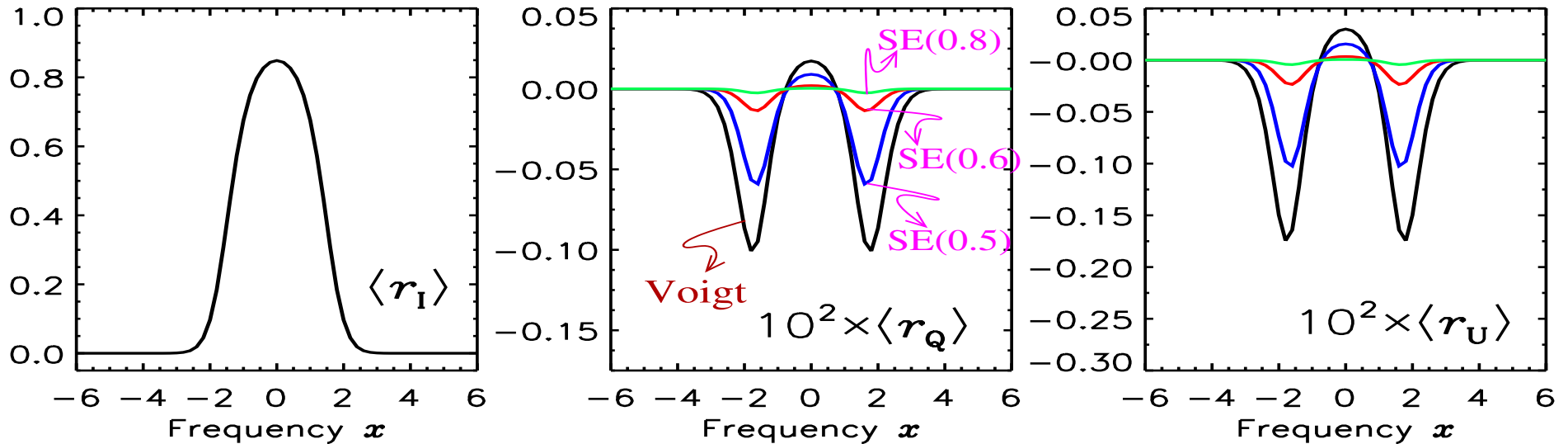
- ★ They show that such a PDF, with  $\Delta_B = 6$  G and  $a_B = 1.5$  best fits the La Palma magnetogram data.

- ★ Stein & Nordlund (2006) propose a Stretched Exponential PDF, derived from magneto-convection simulations :

$$P_{\text{SE}}\left(\frac{B}{\Delta_B}\right) = \frac{k}{2\Gamma(1/k)} e^{-|B/\Delta_B|^k},$$

$k \rightarrow$  is the stretching parameter:  $0 \leq k \leq 1$ .

# Mean solutions computed using Symmetric PDFs



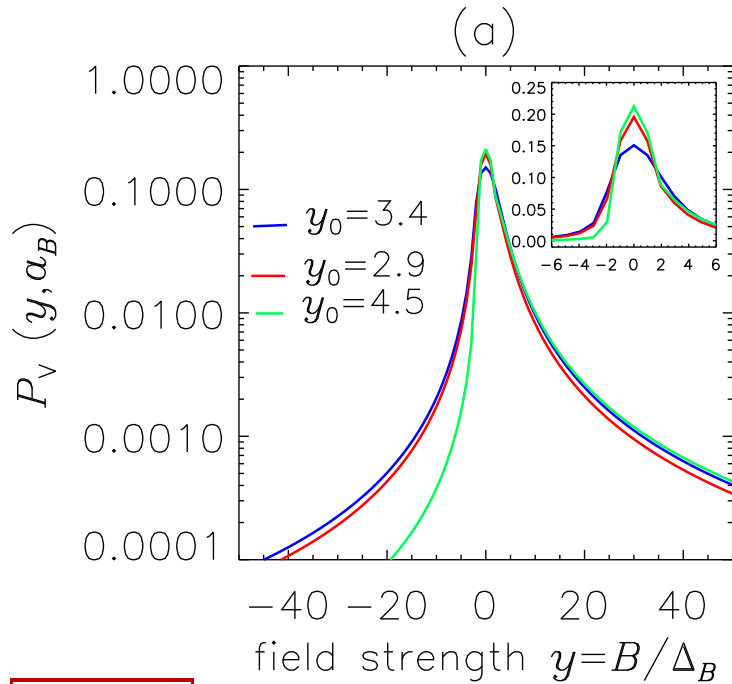
**Model**  $\Delta_B/B_D = 0.0056$ , where  $1/B_D = ge/(4\pi mc\Delta\nu_D)$ ; damping parameter  $a = 0$ ; line strength  $\beta = 10$ ; field orientation  $(\theta, \phi) = (60^\circ, 30^\circ)$ ; correlation length  $(1/\nu = 1/5)$ .

## Results

1.  $\langle r_I \rangle$  is insensitive to the type of PDF, because rms fluctuations =  $\Delta_B/B_D \ll 1$ .
2.  $\langle r_{Q,U} \rangle$  are very sensitive to the type of PDF  $\Rightarrow \therefore$  diagnostically more useful
3. Voigt PDF :- give largest  $\langle r_{Q,U} \rangle$ ,  $\therefore$  strong field tails of  $P_{\text{Voigt}}$  are large.
4.  $P_{\text{SE}}(y)$  :- As  $k$  increases,  $\langle r_{Q,U} \rangle$  decreases  $\therefore$  strong field tails of  $P_{\text{SE}}(y) \rightarrow 0$ .



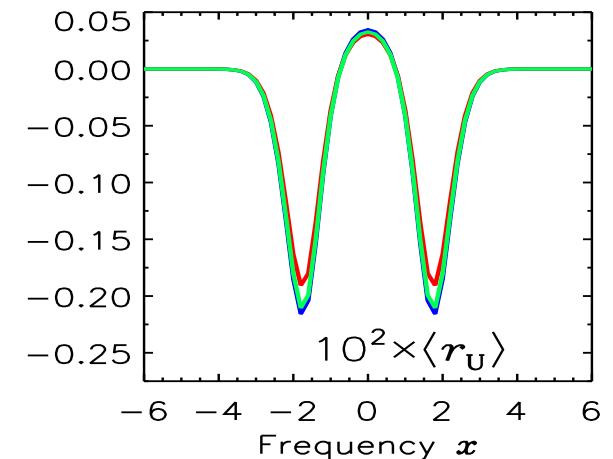
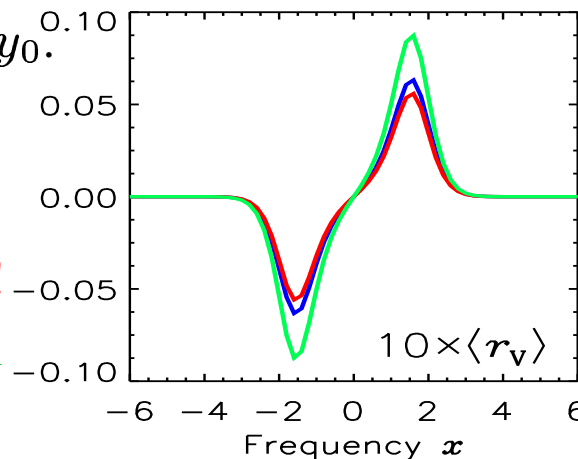
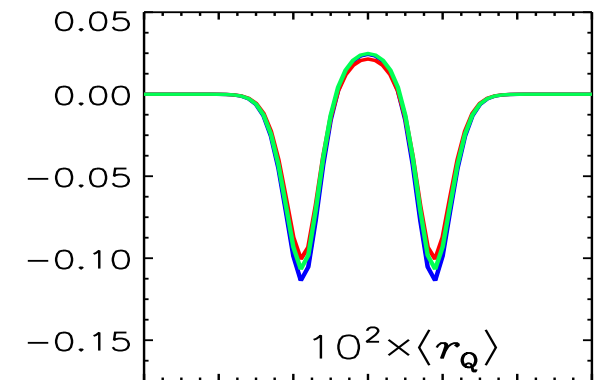
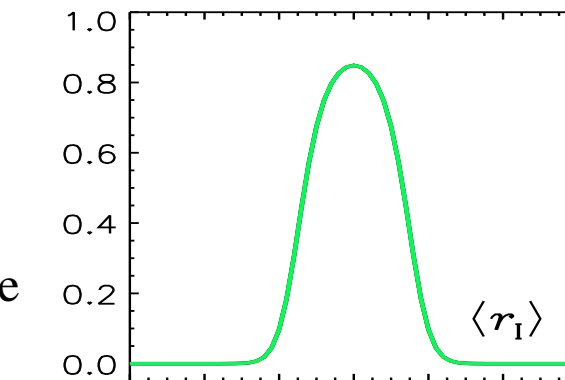
# Asymmetric Voigt PDF (non-zero NET flux)



- ★ Unbalanced NET fields can be generated only by **Asymmetric PDFs**. Symmetric PDFs have zero net flux.
- ★ Asymmetric PDFs are **constructed as follows** :  
use **different  $\alpha_B$**  values for **+ve** and **-ve** polarities ;  
and keep the Gaussian **core symmetric**.
- ★ Asymmetric PDFs have a **non-zero mean field  $y_0$** .

## Results

- $\langle r_{Q,U} \rangle$  are nearly **insensitive** to the asymmetry of the PDFs.
- $\langle r_V \rangle$  peaks at same  $x \approx 1.5$  **for all  $y_0$** .
- The **amplitude** of  $\langle r_V \rangle$  peaks **increases** with the mean field,  
 $\therefore$  it is generated by the **NET flux!**  
 $\langle r_V \rangle$  has larger **diagnostic potential**



# Angular PDFs

- ★ Quiet solar atmosphere is filled with mixed polarity fields.
- ★ Inter-granular lanes contain fields directed either upward or downward.
- ★ Such a scenario can be represented by an angular PDF that has a ‘constant field strength’  $B$  but ‘random orientations’  $(\theta_B, \phi_B)$ :

Ex : power law (see Stenflo 1987) :  $P_{pl}(\mu_B) = [(p+1)/(4\pi)] |\mu_B|^p, \quad -1 \leq \mu_B \leq +1,$

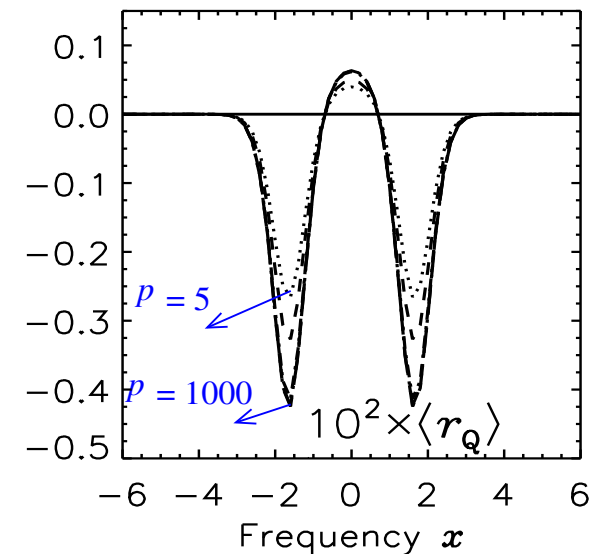
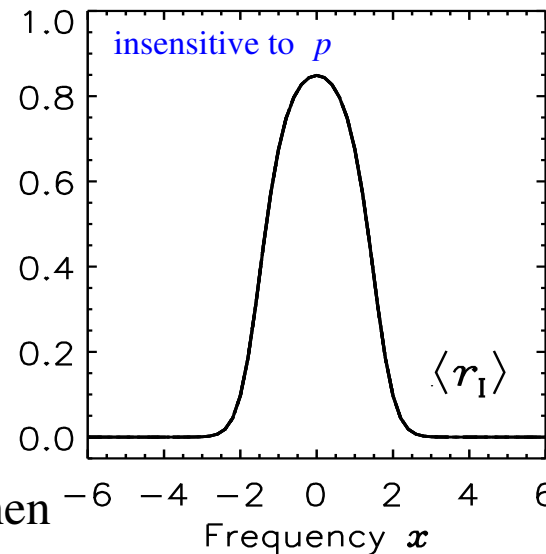
where  $\mu_B = \cos \theta_B$ , with  $\theta_B$  the field orientation with respect to the atmospheric normal.

- ★ When the power law index  $p = 0$  the distribution is isotropic (photospheric like).
- ★ With increasing  $p$  the PDF becomes more and more vertically peaked (flux tube like).

**Model**  $\nu=5$  (meso-turbulent);  
 $B/B_D=0.1; \beta=10; a=0;$   
 $\mu=0.1$  and  $p: 0 \rightarrow 1000$ .

**Results**

1.  $\langle r_Q \rangle \ll \langle r_I \rangle$  ∴ the field is weak.
2.  $\langle r_Q \rangle$  first increases with  $p$  and then saturates (when  $p \simeq 100$ ) to a deterministic solution.



# Composite PDFs that may mimic solar surface fields

- ★ Observation and theory together point to the following facts about the random fields :
  1. Angular variation of the random field should not be the same for all field strength.
  2. PDF should become vertically peaked in the strong field regime (flux tube like).
  3. The “Same” PDF should become isotropic in the weak field regime (photospheric like).
  4. Transition from “isotropic  $\rightarrow$  peaked” distribution should be gradual ( $B_t \approx 50$  G).

★ Based on these facts, we propose 2 composite PDFs (Sampoorna et al. 2008b) :

$$P_{\text{composite}}(\mathbf{B})d\mathbf{B} = \left\{ \begin{array}{l} \overbrace{P_V(B/\Delta_B, a_B) dB/\Delta_B}^{\text{for strength variation}} \star \overbrace{\mu_B^p d\mu_B d\phi_B}^{\text{for angular variation}}, \\ \overbrace{P_{SE}(B/\Delta_B) dB/\Delta_B} \star \overbrace{\mu_B^p d\mu_B d\phi_B}, \end{array} \right.$$

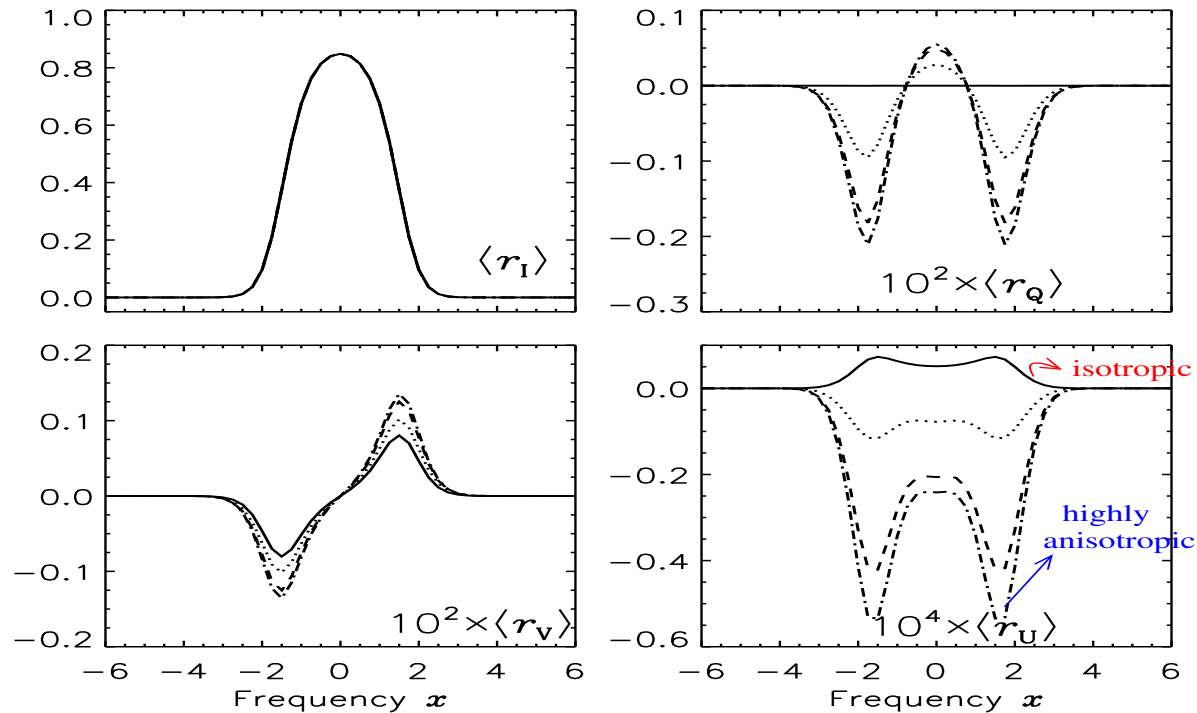
$\mu_B = \cos \theta_B$ , with  $\theta_B =$  orientation w.r.t. the vertical;

power law index  $p = |B|/B_t$ .

$B_t =$  transition field strength between isotropic and peaked distribution ( $\approx 50$  G).

★  $B_t = \infty \Rightarrow p = 0$  and hence  $P_{\text{composite}}$  becomes isotropic distribution for all  $B$ .

# Mean profiles computed with composite PDFs



**Model**  $(a, \beta, \Delta_B/B_D) = (0, 10, 0.0056)$ ; the LOS  $\approx$  parallel to the limb ( $\mu=0.1$ ); asymmetric Voigt PDF with mean field  $y_0=4.5$ ; meso-turbulence ( $\nu=5$ ).

**Line types** [Solid  $y_t=B_t/\Delta_B=\infty$ ] (isotropic), [dotted  $y_t=50$ ], [dashed  $y_t=10$ ], and [dash-dotted  $y_t=5$ ].

**Results** As  $y_t$  decreases, the PDF becomes more and more anisotropic.  $\therefore$  both  $\langle r_{Q,V} \rangle$  increase in magnitude.  $\langle r_U \rangle$  is created purely by magneto-optical effects.

# Conclusions

1. PDFs are well suited to represent in a compact way the randomness of the magnetic field.
2. Asymmetric Voigt PDF is a good choice because the strong field contribution which come from tail regions are correctly represented.
3. We represent a turbulent vector magnetic field by a combination of angular and strength dependent PDFs. Such composite PDFs better describe solar turbulent fields.
4. We formulated and tested few PDFs. They can be used in radiative transfer modeling, simulation, and inversion codes.

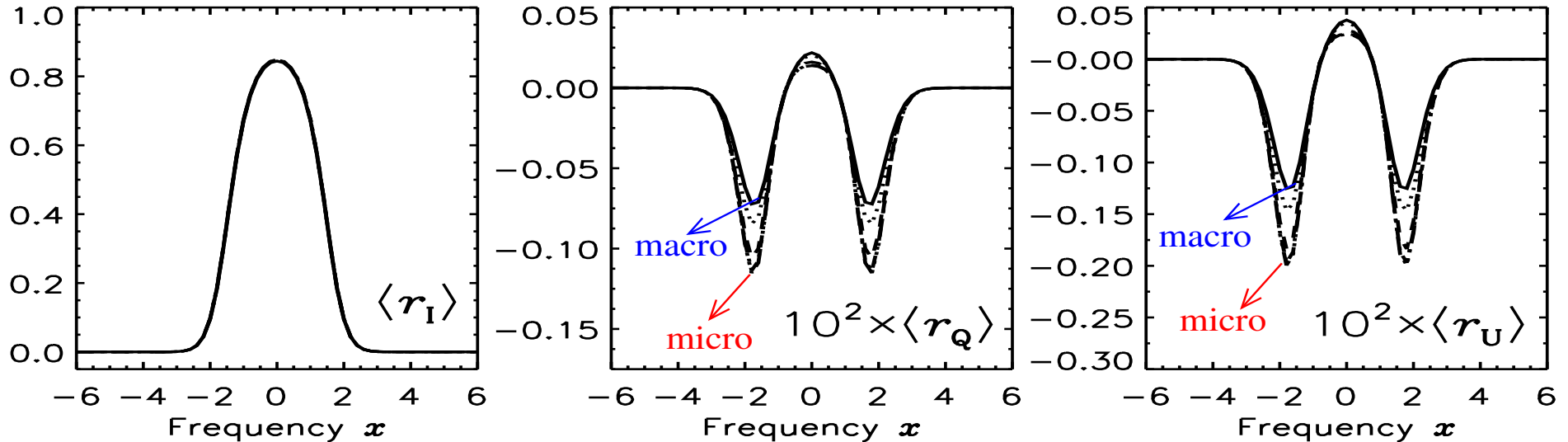
## The Next Steps . . .

1. Turbulence in scattering media (Hanle effect) requires more involved theory. Such a theory is recently formulated by Frisch (2006).
2. We have used Frisch (2006) formulation in radiative transfer calculations with Hanle effect (Frisch, Anusha, Sampoorna, & Nagendra, 2008, in preparation).
3. The effect of different PDFs on Hanle scattered mean Stokes profiles is studied in Anusha et al. (2008, see the poster presented in this conference).

## References

- ▶ Anusha, L. S., Sampoorna, M., Frisch, H., & Nagendra, K. N. 2008, in this proceedings
- ▶ Carroll, T. A., & Kopf, M. 2007, A&A, 468, 323
- ▶ Carroll, T. A., & Staude, J. 2003, Astron. Nachr., 324, 392; 2005, Astron. Nachr., 326, 296
- ▶ Dolginov, A. Z., & Pavlov, G. G. 1972, Soviet Ast., 16, 450
- ▶ Domke, H., & Pavlov, G. G. 1979, Ap&SS, 66, 47
- ▶ Frisch, H., Anusha, L. S., Sampoorna, M., & Nagendra, K. N. 2008, A&A (in preparation)
- ▶ Frisch, H., Sampoorna, M., & Nagendra, K. N. 2006, A&A, 453, 1095
- ▶ Landi Degl'Innocenti, E. 1994, in Solar surface magnetism, eds. R. J. Rutten & C. J. Schrijver (Dordrecht: Kluwer) 29
- ▶ Sánchez Almeida, J., Landi Degl'Innocenti, E., Martinez Pillet, V., & Lites, B. W. 1996, ApJ, 466, 537
- ▶ Sampoorna, M., Nagendra, K. N., & Frisch, H. 2007, JQSRT, 104, 71
- ▶ Sampoorna, M., Frisch, H., & Nagendra, K. N. 2008a, New Astronomy, 13, 233
- ▶ Sampoorna, M., Nagendra, K. N., Frisch, H., & Stenflo, J. O. 2008b, A&A, 485, 275
- ▶ Stein, R. F., & Nordlund, Å. 2006, ApJ, 642, 1246
- ▶ Stenflo, J. O. 1971, in IAU Symp. 43, Solar magnetic fields. Polarized radiation diagnostics, ed. R. Howard, 101
- ▶ Stenflo, J. O. 1973, Solar Physics, 32, 41; 1987, Solar Physics, 114, 1
- ▶ Stenflo, J. O. 2004, Nature, 430, 304
- ▶ Stenflo, J. O., & Holzreuter, R. 2003, Astron. Nachr., 324, 397
- ▶ Trujillo Bueno, J., Shchukina, N., & Asensio Ramos, A. 2004, Nature, 430, 326

# Effect of eddy size ( $\approx 1/\nu$ ) on mean Stokes profiles



**Model** Voigt PDF with  $a_B=1.5$ ;  $\Delta_B/B_D=0.0056$ ;  $a=0$ ;  $\beta=10$ ;  $(\theta, \phi)=(60^\circ, 30^\circ)$ .

**Line types** solid: macro-turbulent ( $\nu=0$ ); dotted ( $\nu=1$ ); dashed ( $\nu=10$ ); dot-dashed ( $\nu=100$ ); and dash triple-dotted: micro-turbulent ( $\nu=200$ ).

**Result I:-** Since  $\Delta_B/B_D \ll 1$ ,  $\langle r_I \rangle$  profiles are insensitive to the eddy size.

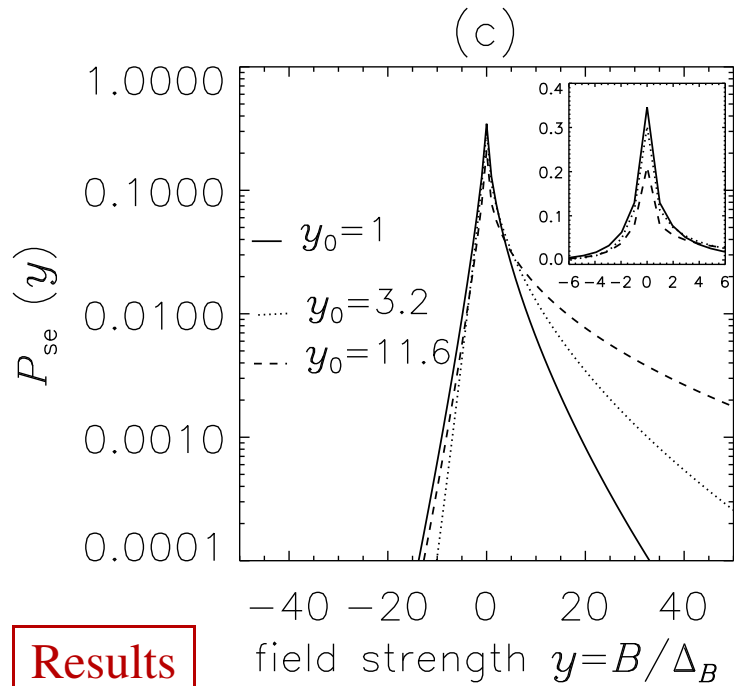
**Result II:-** Meso-turbulent solutions lie between the macro-turbulent ( $\nu = 0$ ; solid) and micro-turbulent ( $\nu = 200$ ; dash triple-dotted) limits.

**Result III:-** Significant differences are observed in the wing peaks of  $\langle r_{Q,U} \rangle$ .

**Result IV:-**  $\langle r_{Q,U} \rangle$  is larger in micro-turbulent case than in macro-turbulent ones.



# Asymmetric Stretched Exp. PDF (non-zero NET flux)



- ★ In this case **asymmetric** PDFs with non-zero  $y_0$  are constructed by choosing **different  $k$**  for **+ve & -ve** polarities.
- ★ **Line types** Solid, dotted, and dashed lines refer to **meso-turbulence**. Heavy dot-dashed line refers to **macro-turbulent limit** (with  $y_0=11.6$ ), for comparison.

## Results

1. **Peak values** of  $\langle r_{Q,U,V} \rangle$  increase with  $y_0$ . **Peak positions** are however insensitive to the mean field  $y_0$ .
2. In  $\langle r_{Q,U} \rangle$  the **differences** between **meso** and **macro**-turbulent profiles are due to **dominance of the +ve tail** of the PDF compared to the -ve.
3.  $\langle r_V \rangle$  is relatively **insensitive to  $\nu$** .

